



# Enhanced solar water splitting of electron beam irradiated titania photoanode by electrostatic spray deposition



Mukund G. Mali<sup>a,1</sup>, Hyun Yoon<sup>a,1</sup>, Seongpil An<sup>a</sup>, Jae-Young Choi<sup>a</sup>, Ha-Yong Kim<sup>a</sup>,  
Byung Cheol Lee<sup>b</sup>, Byung Nam Kim<sup>b</sup>, Ji Hyun Park<sup>b</sup>, Salem S. Al-Deyab<sup>c</sup>, Sam S. Yoon<sup>a,\*</sup>

<sup>a</sup> School of Mechanical Engineering, Korea University, Seoul 136-713, Republic of Korea

<sup>b</sup> Radiation Equipment Research Div., Korea Atomic Energy Res. Inst., Daejeon 305-353, Republic of Korea

<sup>c</sup> Department of Chemistry, College of Science, King Saud University, Riyadh 11451, Saudi Arabia

## ARTICLE INFO

### Article history:

Received 25 April 2014

Received in revised form 10 June 2014

Accepted 13 June 2014

Available online 20 June 2014

### Keywords:

Electrostatic spray deposition

Water splitting

Electron beam

TiO<sub>2</sub>

Thin film

## ABSTRACT

Surface modifications are often made to titania films to improve its photocatalytic performance in water splitting. We herein introduced electron beam irradiation to enhance the photocatalytic activities of an electro-sprayed titania film for solar water splitting application. The film was fabricated by a facile and scalable electrostatic spraying deposition. According to SEM, X-ray diffraction, and Raman data, electron beam densified the film and improved its crystallinity. Absorbance data indicated that the band gap of the E-beam film reduced, which in turn covered the wider range of absorbed light. These modifications increased oxygen vacancies or defects, which enhanced mobility and separation of electrons and holes. As a result, the E-beam film exhibited a threefold increase in the photocurrent density, compared to that of the non-E-beam film. This electro-sprayed titania film was used as a photoanode while the reference and counter electrodes involved in the generation of hydrogen were made of Ag/AgCl and platinum, respectively. The intensity of the UV light illumination used was 1 mW/cm<sup>2</sup>.

© 2014 Elsevier B.V. All rights reserved.

## 1. Introduction

Photoelectrochemical (PEC) cells are capable of harvesting the highly abundant supply of sunlight to produce energy in the form of chemical energy stored within hydrogen, which is produced by water splitting. To trigger photocatalysis, semiconducting materials are needed that can absorb a level of energy equal to or higher than the material's band gap when exposed to photon energy. When this occurs, excited electrons (e<sup>-</sup>) migrate to the conduction band, thus leaving behind holes (h<sup>+</sup>) in the valence band of the semiconductor photoelectrode. Ultimately, these excited electrons travel to the cathode, where they undergo a reduction process, whereas the holes combine with water and produce oxygen at the anode. To achieve higher PEC performance, the top of the valence band (VB) should secure a higher potential than that of oxidation of H<sub>2</sub>O/O<sub>2</sub> (1.23 vs NHE). Similarly, the bottom of the conduction band should secure a lower potential than that of reduction of H<sup>+</sup>/H<sub>2</sub> (0 vs NHE) [1]. The performance of any PEC cell is therefore completely dependent upon the nature of the semiconductor material used

as the photoelectrode. However, the quantum efficiency of this semiconductor is adversely affected by the recombination of holes and electrons. Consequently, in order to achieve better PEC water-splitting performance, the semiconductor photoelectrode should be modified in such a way that it restricts the recombination of electrons and holes.

Titania (TiO<sub>2</sub>) has long been considered one of the most popular semiconducting materials for use in PEC water splitting, due largely to the pioneering work by Fujishima and Honda in 1972 [2]. Since then, titania has been widely accepted for its high physical and chemical stability, greater oxidizing capacity, nontoxic nature, and low price. Furthermore, the band gap energy of titania is suitable for the oxidation and reduction of water, with just a slight modification of the defect chemistry and oxygen stoichiometry all that is required to tune its electronic properties.

Park et al. have previously reported an improved absorption of visible light (>420 nm) after doping of carbon onto TiO<sub>2</sub> nanotube arrays [3]. Similarly, Zhang et al. modified sol-gel synthesized TiO<sub>2</sub> by nitrogen doping in order to improve its photocatalytic activity [4]. Adopting a slightly different approach, Maijenburg et al. successfully synthesized Ag/TiO<sub>2</sub> nanowires to achieve improved water splitting over empty TiO<sub>2</sub> nanotubes [5]. Kumar et al. reported the modification of the work function and surface potential of TiO<sub>2</sub> thin films by exposing them to dense electron excitation

\* Corresponding author. Tel.: +82 2 3290 3376; fax: +82 2 926 9290.

E-mail address: [skyoona@korea.ac.kr](mailto:skyoona@korea.ac.kr) (S.S. Yoon).

<sup>1</sup> These authors contributed equally to this work.

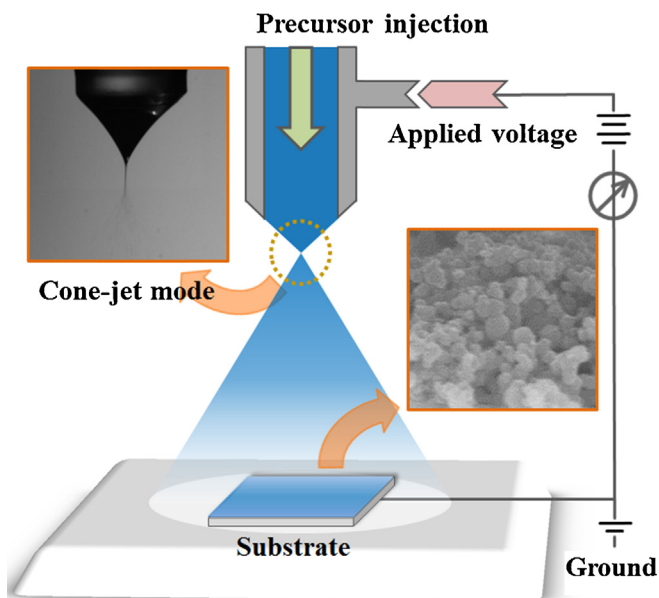


Fig. 1. A schematic for electrostatic spray deposition.

induced by a 100 MeV Ni ion beam [6]. Later, Yun et al. reported improved electronic and optical properties in nanomaterials following irradiation by energy electron beam [7–9]. Electron beam irradiation therefore presents a novel and potentially very valuable tool for the engineering and modification of materials at an atomic level. In this way, various functional properties and electronic structures can be achieved by tuning selected oxides with energy electron beam irradiation. Improvements in the electronic structure are made possible by the formation of defects such as oxygen vacancies in the bulk material.

In this study,  $\text{TiO}_2$  thin-film photoelectrodes were prepared by electrostatic spray deposition (ESD), and then subjected to low-energy (0.2 MeV) electron beam irradiation in an effort to optimize their performance in PEC water splitting. As depicted in Fig. 1, ESD is an attractive option for preparing a uniform film as it yields extremely fine, self-dispersive, highly wettable, adhesive droplets [10]. Moreover, ESD is capable of producing pure materials with structural control at a nanometer scale. The crystallinity, surface texture, film thickness, and deposition rate can therefore all be easily controlled by adjusting the voltage, flow rate, precursor concentration, and substrate temperature [10]. In ESD, charged droplets are accelerated toward a substrate, thereby offering improved targeting and resulting in a high deposition efficiency and low material consumption [11–13]. To the best of our knowledge, there have yet been no reports pertaining to the effect of electron beams on electro sprayed titania films intended for use in PEC water splitting. Consequently, the changes in the physico-chemical structure of  $\text{TiO}_2$  films after electron beam irradiation and their subsequent mechanism of PEC water splitting are investigated herein in detail.

## 2. Experimental

### 2.1. Titania films

A spray solution was first prepared by mixing titanium tetraisopropoxide (TTIP,  $\text{Ti}[\text{OCH}(\text{CH}_3)_2]_4$ , 97%, Sigma–Aldrich) with deionized water, ethyl alcohol ( $\text{C}_2\text{H}_5\text{OH}$ , 99.9%, Duksan chemical), and DEG ( $\text{C}_4\text{H}_{10}\text{O}_3$ , Duksan chemical) to the amount of 1, 1.5, 50, and 50 ml, respectively. This solution was stirred at room temperature, and then the ethanol was evaporated by heating it to 80 °C.

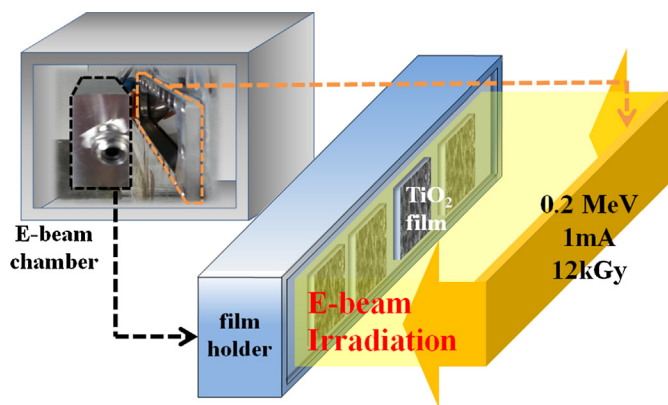


Fig. 2. A schematic for electron beam irradiation.

The resulting ethanol-free precursor was used to form a stable Taylor cone for ESD, being electrostatically sprayed at 1 ml/h onto an indium tin oxide (ITO)-coated conductive glass substrate at 230 °C for 20 min. Finally, the as-prepared films were annealed for 10 min at 500 °C in a closed furnace.

### 2.2. Electron beam irradiation

An electron beam typically consists of low-energy electrons, its irradiation on to a material inducing a variety of changes in its original properties. To this end, the electrostatically sprayed  $\text{TiO}_2$  films were irradiated under ambient conditions with a low-energy (0.2 MeV, 1 mA) electron beam at the Korea Atomic Energy Research Institute (KAERI, Daejeon, Korea). For uniform deposition, titania films were mounted on a sample holder located at 2 cm downstream of the electron beam window. The irradiation time is proportional to the amount of electron beam. This irradiation is depicted schematically in Fig. 2, with each sample absorbing a dose equivalent to 12 kGy.

### 2.3. Characterization

The structural aspects of pure  $\text{TiO}_2$  films and the low-energy electron beam-irradiated  $\text{TiO}_2$  films were studied using X-ray diffraction (XRD, Rigaku, Japan, D/max-2500) with  $\text{CuK}\alpha$  radiation over a  $2\theta$  range of 10–70°. Raman measurements were also performed using a confocal Raman spectrometer (NRS-3100) with a 514 nm laser excitation source. The surface chemical composition of the titania films was studied by X-ray photoelectron spectroscopy (XPS, Theta Probe base system, Thermo Fisher Scientific Co.), whereas UV–visible spectrometry (Optizen POP Mecasys Co. Ltd, Korea) was used to study their absorbance. The surface morphology of the films was studied by scanning electron microscopy (HR-SEM, XL30 SFEG, Phillips Co., Holland) at 10 kV, the film thickness being determined from an average of five different measurements so as to yield statistically reliable data.

For all photoelectrochemical measurements, a single cell with a three-electrode set-up was used. Fig. 3 shows a schematic of the PEC setup used, in which pure and electron beam-treated films were used as the working electrode (anode). To complete the set-up, Ag/AgCl rod was used as the reference electrode, and a platinum wire was used as the counter electrode (cathode). All of the electrodes were kept as close as possible to each other, and their locations were kept constant for all measurements. A solution of 1.0M KOH (pH = 14) was used as the electrolyte, with this being purged with nitrogen to remove any dissolved oxygen prior to testing. A 400 W xenon arc lamp (Newport, Oriel Instruments, USA) was used to provide a light intensity of 1 mW/cm<sup>2</sup>. A water filter

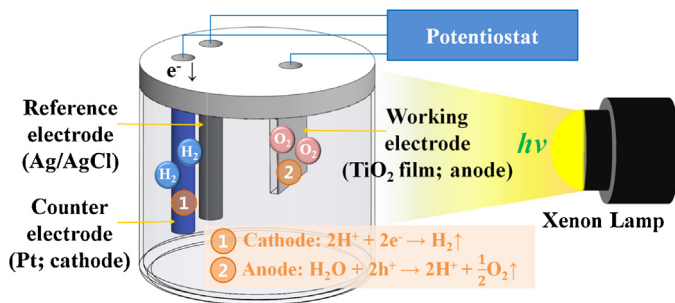


Fig. 3. A schematic for photoelectrochemical water splitting.

was used to reduce output in the IR region, while allowing through all UV light with a wavelength lower than 420 nm.

### 3. Results and discussion

#### 3.1. Physicochemical structure of the films

The effect of low-energy beam irradiation on the structure of  $\text{TiO}_2$  thin films was evaluated on the basis of several physicochemical characterizations. Fig. 4 shows the XRD spectra for pure and low-energy electron beam irradiated  $\text{TiO}_2$  thin films prepared by electrostatic spray deposition. It should be noted that the pure  $\text{TiO}_2$  film was annealed at  $500^\circ\text{C}$ . Pattern for the pure  $\text{TiO}_2$  film exhibits moderate diffraction peaks at  $2\theta$  angles of  $25.04$ ,  $37.52$ ,  $47.84$ ,  $53.76$ ,  $54.70$  and  $62.28^\circ$ , which correspond to the  $101$ ,  $004$ ,  $200$ ,  $105$ ,  $211$  and  $204$  planes, respectively. By comparing these peaks against JCPDS file #21-1272, it is confirmed that the  $\text{TiO}_2$  film consists solely of an anatase phase. Fig. 4 also depicts the XRD patterns of the  $\text{TiO}_2$  thin films after low-energy electron beam irradiation, from which it is evident that these films display far more sharp and highly intense peaks than pure  $\text{TiO}_2$ . This indicates an increase in the crystallinity of the films that is attributed to the localized temperature increase within the film during irradiation, which is likely to result in a rearrangement of atoms. Indeed, a very similar result was obtained by Dhawale et al. for chemically deposited  $\text{TiO}_2$  nanorods [14].

This increased crystallinity of the  $\text{TiO}_2$  film after irradiation is further confirmed by the Raman spectroscopy results. Fig. 5 shows the distinct Raman peaks attributed to the anatase phase of  $\text{TiO}_2$  [14]. In general, the anatase phase of  $\text{TiO}_2$  is characterized by six modes of Raman comprising one  $A_{1g}$ , two  $B_{1g}$  and three  $E_g$  modes. In the present work, five Raman modes (except one  $B_{1g}$ ) are observed,

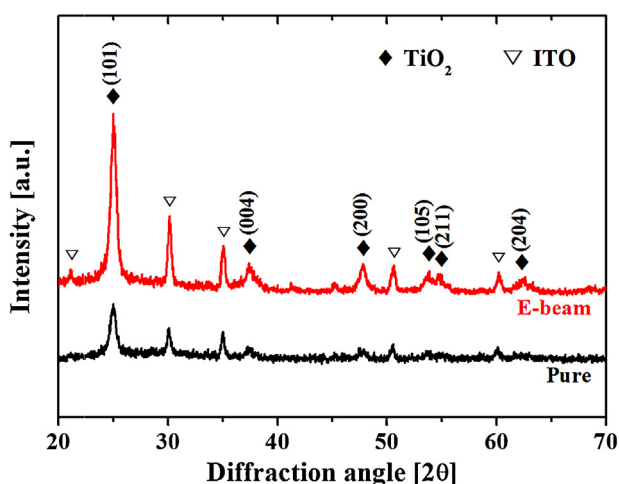


Fig. 4. XRD spectra for pure and E-beam films.

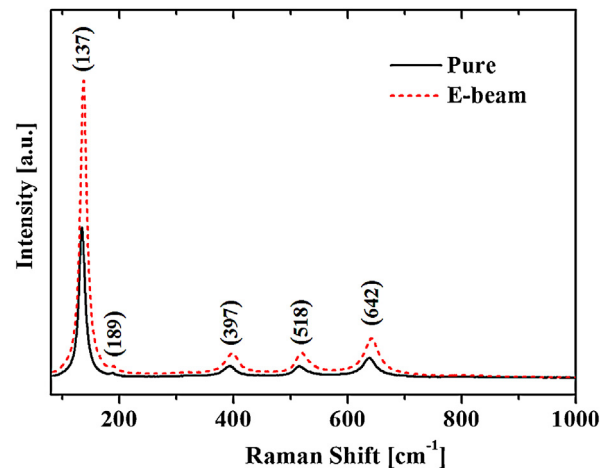


Fig. 5. Raman spectra for pure and E-beam films.

as shown in Fig. 5. Raman peaks of the E-beam irradiated  $\text{TiO}_2$  thin film show a markedly increased intensity, which confirms an increase in the crystalline nature of the film. The most intense peak after irradiation is observed near  $137\text{ cm}^{-1}$ , and corresponds to the  $E_g$  vibrational mode, which is caused by the O–Ti–O symmetric stretching vibrations [15]. Since this peak exhibits a slight high-field shift, it indicates that there is a higher degree of oxygen vacancies [16]. Consequently, considerable information regarding structural changes in the material can be derived by exploring this region [17].

The composition of the  $\text{TiO}_2$  thin films was determined by XPS analysis. Fig. 6 shows the XPS spectra of pure and electron-beam irradiated  $\text{TiO}_2$  thin films. The result that the  $\text{Ti}2p$  spectrum of the  $\text{TiO}_2$  film (Fig. 6a) exhibits characteristic  $2p_{3/2}$  and  $2p_{1/2}$  photoelectron peaks at  $458.38$  and  $464.18\text{ eV}$  respectively [18]. However, when the  $\text{TiO}_2$  film is irradiated, these  $2p_{3/2}$  and  $2p_{1/2}$  peaks are shifted toward a higher binding energies; being observed at  $458.53$  and  $464.38\text{ eV}$ , respectively. Such a shift toward higher binding energies can be attributed to band tuning, which is commonly observed in metal oxides [19,20]. Note that “tuning” herein refers to the tuning of the valence band (VB) and conduction band (CB) by means of electron beam irradiation. Furthermore, there is also the distinct possibility for Ti–O–Ti bonds to be formed in the film structure [21]. Carbon is present in the films as an impurity, as evidenced by the C  $1s$  spectra of the pure and irradiated  $\text{TiO}_2$  thin-films shown in Fig. 6b. The decrease in the intensity of this C  $1s$  peak after irradiation is consistent with the results of Kim et al. [22], and is attributed to the partial oxidation of the carbon content of the film. This means that although there is a deposition of hydrocarbons from air onto the film surface during irradiation, at the same time there is a removal of carbon from the film surface. Since the rate of removal is greater than rate of deposition, the overall carbon content of the irradiated film is less, as evidenced by the less intense C  $1s$  peak. Finally, Fig. 6c shows peaks corresponding to lattice oxygen of pure and irradiated  $\text{TiO}_2$  at  $529.58$  and  $529.78\text{ eV}$  respectively.

#### 3.2. Optical properties of the films

From a study of the physicochemical structure of the electro-sprayed  $\text{TiO}_2$  thin-films after electron beam irradiation, it was found that defects were created in the  $\text{TiO}_2$  matrix. Hence, in order to assess their effect on the optical properties of the films, UV–visible absorbance spectra were recorded both before and after irradiation. As can be seen from Fig. 7, a red-shift occurs in the absorbance spectrum of  $\text{TiO}_2$  thin-films subjected to irradiation,

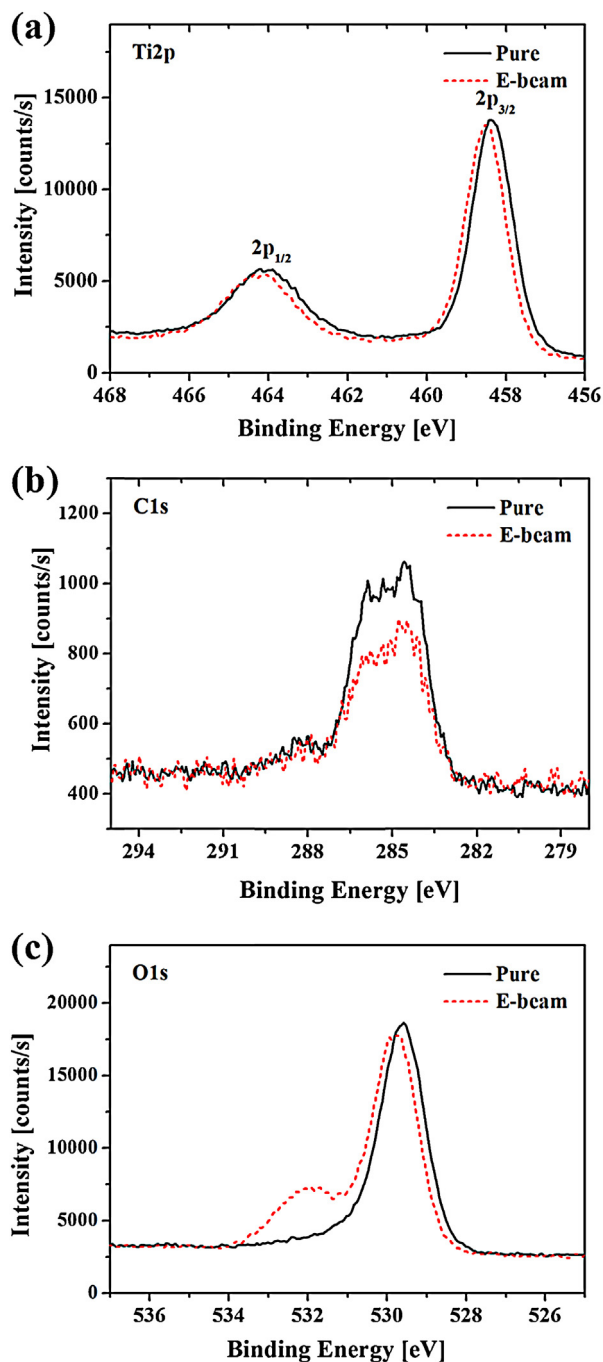


Fig. 6. XPS spectra of (a) Ti 2p, (b) C 1s and (c) O 1s for pure and E-beam films.

which indicates a decrease in the band gap energy that is credited to the creation of defects such as oxygen vacancies [23]. It is worth noting that this decrease in band gap is directly proportional to the photocatalytic activity. The band gap reduction after irradiation suggests that the film can absorb the wider range of spectrum of light, resulting in generation of more number of electron–hole pairs. Thus, the irradiated films are expected to exhibit an enhanced photocatalytic activity (i.e., photocurrent density).

### 3.3. Surface morphology and film thickness

The effect of low-energy electron beam irradiation on the morphology of the TiO<sub>2</sub> thin films was evaluated by SEM. Fig. 8a and b shows a top view and cross-sectional view of a pure TiO<sub>2</sub> film,

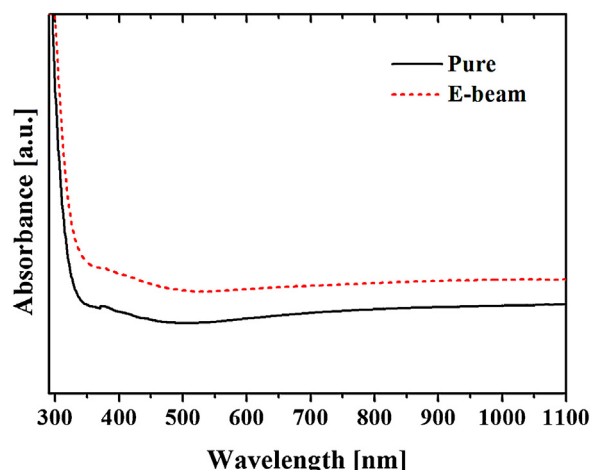


Fig. 7. UV–visible absorbance of pure and E-beam films.

while Fig. 8c and d shows a top view and cross-sectional view of an irradiated TiO<sub>2</sub> film. It is evident that electron beam irradiation has a strong influence on the microstructure of a TiO<sub>2</sub> film. For instance, a pure TiO<sub>2</sub> film shows a somewhat smooth and porous morphology with a uniform distribution of TiO<sub>2</sub> nanoparticles. In contrast, the irradiated TiO<sub>2</sub> film is denser and rougher (Fig. 8c) with a more irregular microstructure. Moreover, the thickness of the film is reduced by irradiation from  $\sim 5 \mu\text{m}$  in the case of pure TiO<sub>2</sub> film (Fig. 8b), to  $\sim 3 \mu\text{m}$ . This can be explained by the fact that when highly energetic electrons collide with the TiO<sub>2</sub> film surface, they produce local or transient high-energy states. This energy in turn dissipated by collision with other electrons, resulted in a localized heating of the atomic system. It is therefore quite plausible that electron beam irradiation results in partial melting of TiO<sub>2</sub> with subsequent recrystallization during quenching forming a dense and rough hillock structure.

### 3.4. Photoelectrochemical performance

From the structural, optical and morphological characterizations, it has been shown that low-energy electron beam irradiation significantly affects the physicochemical properties of an electrostatic-spray-deposited TiO<sub>2</sub> film. The photocurrent stability under illumination was assessed as a standard measure for the water splitting performance of photoelectrodes, which directly corresponds to oxygen evolution.

Fig. 9 shows the effect of low-energy electron beam irradiation on the current–potential ( $J$ – $V$ ) curves (photocurrent density) of ESD TiO<sub>2</sub> thin films. The photocurrent densities of both pure and irradiated TiO<sub>2</sub> thin films are negligible when they are not illuminated in a dark condition (not shown herein), but show an enhanced photoresponse when illuminated by UV light with an intensity of  $1 \text{ mW}/\text{cm}^2$ . The photocurrent onset potential is at around  $-0.9 \text{ V}$  vs Ag/AgCl, with the pure TiO<sub>2</sub> film exhibiting a stable photocurrent of  $\sim 40 \mu\text{A}/\text{cm}^2$  from  $-0.2 \text{ V}$  of applied potential. In contrast, the irradiated films show a dramatic threefold increase in the photocurrent density, reaching a maximum of  $\sim 115 \mu\text{A}/\text{cm}^2$  at  $-0.2 \text{ V}$ . Hence, electron beam irradiation significantly enhances the photocurrent density of electrostatically deposited TiO<sub>2</sub> thin films, with such a dramatic increase attributed to the favorable physicochemical changes induced in the film. The separation and mobility of the carrier charges is crucial, which determines the rate of photocatalytic reaction.

In photocatalysis, mobility and separation of photo-excited electrons and holes dominate the overall energy conversion efficiency of the solar water splitting process. These activities of carrier

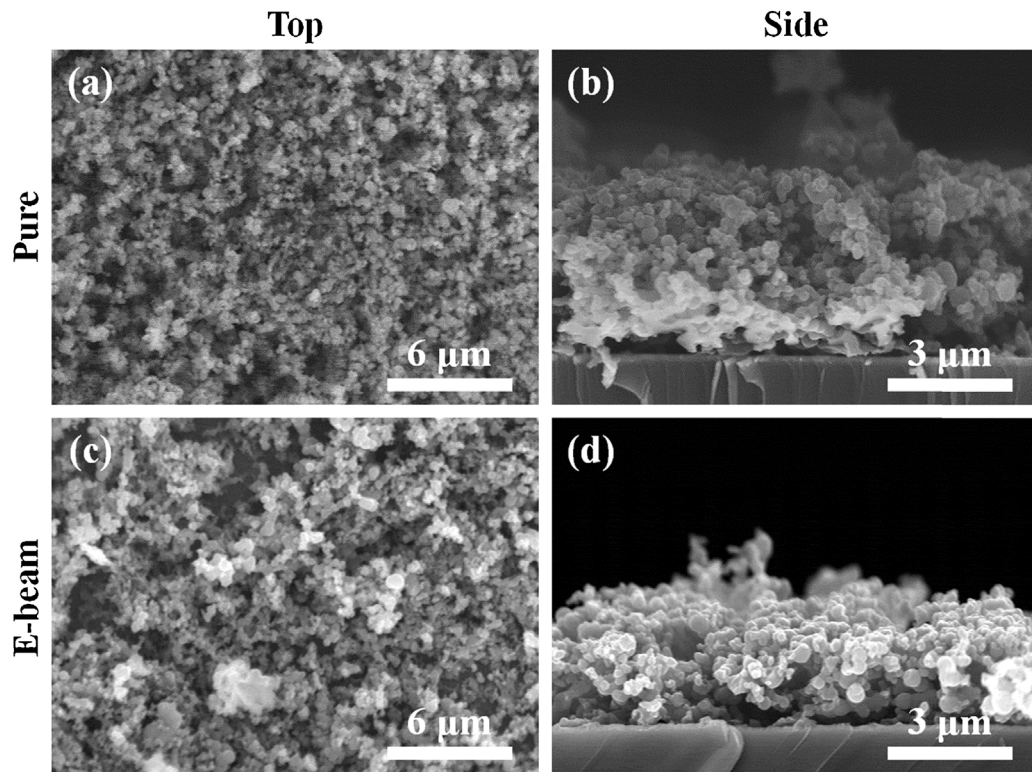


Fig. 8. SEM images of (a), (b) pure and (c), (d) E-beam films.

charges are enhanced when the film bulk is subject to more defects or oxygen vacancies [24]. Electron beam serves to create such defects in the film. For example, it is known that a low-energy electron beam can desorb oxygen ions and neutral atoms from the surface of  $\text{TiO}_2$ , which leads to the generation of vacancies [25,26]. Hence, defects can be created in a  $\text{TiO}_2$  thin-film without causing damage, by using a moderate beam energy to generate oxygen vacancies [27]. The generation of a large number of defects leads to the formation of shallow traps within the  $\text{TiO}_2$  matrix that prevent the recombination of photogenerated electron–hole pairs, thereby improving PEC performance [28]. This is further supported by the work of Jun et al., in which an increased concentration of  $\text{Ti}^{3+}$  and oxygen vacancies was observed as a result of low-energy

electron beam bombardment, thereby causing a reduction in the electron–hole pair recombination rate [29].

Low-energy electron beam irradiation also has a major impact in reducing the thickness of  $\text{TiO}_2$  films. The advantage of the denser film is that when a  $\text{TiO}_2$  film is illuminated with UV light of a desired wavelength (i.e., with an energy greater than its band gap), electrons ( $e^-$ ) generated in the valence band travel to the conduction band, thereby leaving holes ( $h^+$ ) in the valence band more efficiently. Both these generated electrons and holes migrate to the surface of the  $\text{TiO}_2$ . The migration of electrons and holes could be influenced by the film densification, which reduces the recombination rate via efficient transport of charge carriers ( $e^-$  and  $h^+$ ).

To reassure the dominant favorable effect of E-beam, Fig. 9 compares the photocurrent density (PCD) values of the pure films having 3 and 5  $\mu\text{m}$  against that of the E-beam film. It is clear that the E-beam film is superior to the other two films in terms of the PCD value while having 115  $\mu\text{A}/\text{cm}^2$  at  $-0.2\text{ V}$  vs  $\text{Ag}/\text{AgCl}$ . Roughness and densification of the film resulting from E-beam yielded the environment for efficient electron mobility. On the other hand, we also noticed that film thickness did not play a significant role in PCD while comparing the PCD of the pure films of two different thicknesses of 3 and 5  $\mu\text{m}$ . However, the slightly greater PCD value of the thicker film may imply that the greater surface area enhanced the photocatalytic activity though the PCD difference was minor. At present, there are few reports in the literature that directly concern the use of low-energy electron beam irradiation for improving the PEC or photocatalytic performance of semiconductor photoanodes, and thus this technique has great future potential for the field of photoelectrochemistry.

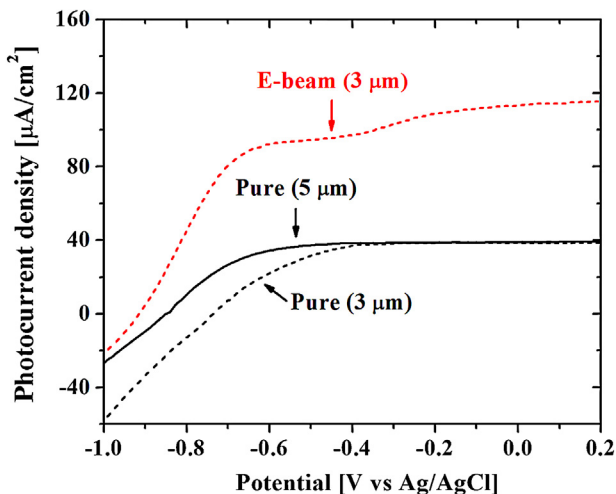


Fig. 9. Photocurrent vs potential curves of the pure and E-beam films.

#### 4. Conclusion

We conclusively demonstrated that the photoactivity of an electrosprayed titania film, suitable for use in PEC water splitting, could be greatly enhanced by the use of electron beam irradiation. These

electron beam-treated films showed a nearly threefold increase in photocurrent density, which was explained by the creation of oxygen vacancies. An improvement in crystallinity was also observed via XRD, Raman and XPS analyses. Moreover, an observed red-shift in the UV spectra of the electron beam-treated film suggested an enhanced light absorption. With the low cost deposition method such as electrospraying, the electron beam titania film may be an alternative route to the commercialization of solar water splitting.

### Acknowledgments

This work was supported by the Human Resources Development program (KETEP-20124030200120) and by NRF-2014M2B2A4030509. The Authors extend their appreciation to the Deanship of Scientific Research at King Saud University for funding the work through the research group project No. RGP-VPP-089

### References

- [1] R.M. Navarro, M.C. Alvarez-Galván, J.A. Villoria de la Mano, S.M. Al-Zahrani, J.L.G. Fierro, A framework for visible-light water splitting, *Energy Environ. Sci.* 3 (2010) 1865–1882.
- [2] A. Fujishima, K. Honda, Photolysis–decomposition of water at the surface of an irradiated semiconductor, *Nature* 238 (1972) 37–38.
- [3] J.H. Park, S. Kim, A.J. Bard, Novel carbon-doped TiO<sub>2</sub> nanotube arrays with high aspect ratios for efficient solar water splitting, *Nano Lett.* 6 (2006) 24–28.
- [4] Z. Zhang, X. Wang, J. Long, Q. Gu, Z. Ding, X. Fu, Nitrogen-doped titanium dioxide visible light photocatalyst: spectroscopic identification of photoactive centers, *J. Catal.* 276 (2010) 201–214.
- [5] A.W. Maijenburg, J. Veerbeek, R. de Putter, S.A. Veldhuis, M.G.C. Zoontjes, G. Mul, J.M. Montero-Moreno, K. Nielsch, H. Schäfer, M. Steinhart, J.E. ten Elshof, Electrochemical synthesis of coaxial TiO<sub>2</sub>–Ag nanowires and their application in photocatalytic water splitting, *J. Mater. Chem. A* 2 (2014) 2648–2656.
- [6] A. Kumar, M.K. Jaiswal, D. Kanjilal, R.K. Joshi, T. Mohanty, Fermi level shifting of TiO<sub>2</sub> nanostructures during dense electronic excitation, *Appl. Phys. Lett.* 99 (2011) 013109.
- [7] E.-J. Yun, J.W. Jung, K.N. Ko, J. Hwang, B.C. Lee, M.-H. Jung, Effect of high-energy electron beam irradiation on the properties of AZO thin films prepared by RF magnetron sputtering, *Thin Solid Films* 518 (2010) 6236–6240.
- [8] E.-J. Yun, J.W. Jung, Y.H. Han, M.-W. Kim, B.C. Lee, Effect of high-energy electron beam irradiation on the properties of ZnO thin films prepared by magnetron sputtering, *J. Appl. Phys.* 105 (2009) 123509.
- [9] E.-J. Yun, J.W. Jung, Y.H. Han, M.-W. Kim, B.C. Lee, Effect of high-energy electron beam irradiation on the transmittance of ZnO thin films on transparent substrates, *J. Korean Phys. Soc.* 56 (2010) 356–361.
- [10] H. Yoon, J.H. Woo, Y.M. Ra, S.S. Yoon, H.Y. Kim, S. Ahn, J.H. Yun, J. Gwak, K. Yoon, S.C. James, Electrostatic spray deposition of copper–indium thin films, *Aerosol Sci. Technol.* 45 (2011) 1448–1455.
- [11] H. Yoon, J.H. Woo, B. Joshi, Y.M. Ra, S.S. Yoon, H.Y. Kim, S.J. Ahn, J.H. Yun, J. Gwak, K.H. Yoon, S.C. James, CuInSe<sub>2</sub> (CIS) thin film solar cells by electrostatic spray deposition, *J. Electrochem. Soc.* 159 (2012) H444–H449.
- [12] H. Yoon, B. Joshi, S.H. Na, S.S. Yoon, Antibacterial activity and photocatalysis of electrosprayed titania films, *J. Electrochem. Soc.* 159 (2012) H823–H827.
- [13] T. Ohsaka, F. Izumi, Y. Fujiki, Raman-spectrum of anatase, TiO<sub>2</sub>, *J. Raman Spectrosc.* 7 (1978) 321–324.
- [14] D.S. Dhawale, D.P. Dubal, R.R. Salunkhe, T.P. Gujar, M.C. Rath, C.D. Lokhande, Effect of electron irradiation on properties of chemically deposited TiO<sub>2</sub> nanorods, *J. Alloys Compd.* 499 (2010) 63–67.
- [15] J. Yan, G. Wu, N. Guan, L. Li, Z. Li, X. Cao, Understanding the effect of surface/bulk defects on the photocatalytic activity of TiO<sub>2</sub>: anatase versus rutile, *Phys. Chem. Chem. Phys.* 15 (2013) 10978–10988.
- [16] H.-J. Kim, M.-K. Han, S.-M. Lee, D.K. Hwang, Y.-G. Shul, Characterization of Au/MnO<sub>x</sub>/TiO<sub>2</sub> for photocatalytic oxidation of carbon monoxide, *Top. Catal.* 47 (2008) 109–115.
- [17] P. Romerogomez, A. Palmero, F. Yubero, M. Vinnichenko, A. Kolitsch, A. Gonzalez-Eliphe, Surface nanostructuring of TiO<sub>2</sub> thin films by ion beam irradiation, *Scripta Mater.* 60 (2009) 574–577.
- [18] L. Ge, M. Xu, Fabrication and characterization of TiO<sub>2</sub> photocatalytic thin film prepared from peroxo titanic acid sol, *J. Sol–Gel Sci. Technol.* 43 (2007) 1–7.
- [19] B. Reddy, B. Chowdhury, P. Smirniots, An XPS study of the dispersion of MoO<sub>3</sub> on TiO<sub>2</sub>–ZrO<sub>2</sub>, TiO<sub>2</sub>–SiO<sub>2</sub>, TiO<sub>2</sub>–Al<sub>2</sub>O<sub>3</sub>, SiO<sub>2</sub>–ZrO<sub>2</sub>, and SiO<sub>2</sub>–TiO<sub>2</sub>–ZrO<sub>2</sub> mixed oxides, *Appl. Catal. A: Gen.* 211 (2001) 19–30.
- [20] R. Reiche, S. Oswald, F. Yubero, J.P. Espinos, J.P. Holgado, A.R. Gonzalez-Eliphe, Monitoring interface interactions by XPS at nanometric tin oxides supported on Al<sub>2</sub>O<sub>3</sub> and Sb<sub>2</sub>O<sub>3</sub>, *J. Phys. Chem. B* 108 (2004) 9905–9913.
- [21] K. Hayashi, M. Takahashi, K. Nomiya, Novel Ti–O–Ti bonding species constructed in a metal-oxide cluster, *Dalton Trans.* (2005) 3751–3756.
- [22] M.J. Kim, K.-D. Kim, W.S. Tai, H.O. Seo, Y. Luo, Y.D. Kim, B.C. Lee, O.K. Park, Enhancement of photocatalytic activity of TiO<sub>2</sub> by high-energy electron-beam treatment under atmospheric pressure, *Catal. Lett.* 135 (2010) 57–61.
- [23] M.M. Khan, S.A. Ansari, D. Pradhan, M.O. Ansari, D.H. Han, J. Lee, M.H. Cho, Band gap engineered TiO<sub>2</sub> nanoparticles for visible light induced photoelectrochemical and photocatalytic studies, *J. Mater. Chem. A* 2 (2014) 637–644.
- [24] S.A. Ansari, M.M. Khan, S. Kalathil, A. Nisar, J. Lee, M.H. Cho, Oxygen vacancy induced band gap narrowing of ZnO nanostructures by an electrochemically active biofilm, *Nanoscale* 5 (2013) 9238–9246.
- [25] L.-Q. Wang, D.R. Baer, M.H. Engelhard, A.N. Shultz, The adsorption of liquid and vapor water on TiO<sub>2</sub> (1 1 0) surfaces: the role of defects, *Surf. Sci.* 344 (1995) 237–250.
- [26] S. Eriksen, R. Egdell, Electronic excitations at oxygen deficient TiO<sub>2</sub> (1 1 0) surfaces: a study by EELS, *Surf. Sci.* 180 (1987) 263–278.
- [27] X. Pan, M.Q. Yang, X. Fu, N. Zhang, Y.J. Xu, Defective TiO<sub>2</sub> with oxygen vacancies: synthesis, properties and photocatalytic applications, *Nanoscale* 5 (2013) 3601–3614.
- [28] M.S. Kim, W.J. Jo, D. Lee, S.-H. Baeck, J.H. Shin, B.C. Lee, Enhanced photocatalytic activity of TiO<sub>2</sub> modified by e-beam irradiation, *Bull. Korean Chem. Soc.* 34 (2013) 1397–1400.
- [29] J. Jun, M. Dhayal, J.-H. Shin, J.-C. Kim, N. Getoff, Surface properties and photoactivity of TiO<sub>2</sub> treated with electron beam, *Radiat. Phys. Chem.* 75 (2006) 583–589.